# Magnetization Reversal in Ultrathin Films with Monolayer-Scale Surface Roughness

A. Moschel,* R. A. Hyman, and A. Zangwill

*School of Physics, Georgia Institute of Technology, Atlanta, Georgia 30332*

M. D. Stiles

*Electron Physics Group, National Institute of Standards and Technology, Gaithersburg, Maryland 20899*

(Received 15 April 1996)

The intrinsic anisotropy of nominally flat, ultrathin ferromagnetic films typically is augmented by a uniaxial anisotropy at step edges. We report model calculations of hysteresis for such systems with in-plane magnetization and monolayer-scale roughness. The reversal process is a combination of domain nucleation at step edges, expansion of these domains through morphological constrictions, and coherent rotation within domains. The initiation of reversal at well separated step edges can explain the very small coercive fields measured for real ultrathin magnetic films.    [S0031-9007(96)01544-X]

PACS numbers: 75.70.−i, 75.60.−d

Ultrathin film magnetism has evolved into a mature field of study over the past fifteen years [1]. Two-dimensional critical phenomena provided much early motivation, but considerable interest and activity now focuses on the complexities of exchange coupling and anisotropy in order to understand the unusual hysteresis loops commonplace in magnetic multilayers. Insight has been gained from even the simplest models of magnetization reversal [2], where one assumes perfectly flat interfaces, and the coherent rotation model of Stoner and Wohlfarth [3]. Typical generalizations examine some effects of interface roughness within the coherent rotation model [4] or consider the effects of inhomogeneous magnetization reversal within the flat interface model [5]. But as Arrott [6] has pointed out, there is an intimate connection between roughness and reversal that has been insufficiently explored for both simple and multilayer films.

Our calculations are motivated by the steadily accumulating experimental evidence that growth-induced surface roughness can profoundly affect magnetization reversal and coercivity in ultrathin films [7]. Scanning tunneling microscopy graphically demonstrates that roughness at the monolayer scale is the best that can be achieved for any coverage of deposited material [8]. For this reason, even the best as-grown or annealed ultrathin films have some step edges associated either with the perimeter of monolayer-height islands that nucleate during growth or with the steps of an intentionally miscut substrate. This is significant because the magnetic anisotropy at sites of reduced crystallographic symmetry can compete successfully with the intrinsic anisotropy of the flat surface and thereby control coercivity and magnetization reversal [6]. Measurements for magnetic films grown on vicinal substrates add force to this general argument [9].

In this paper, we study magnetization reversal at $T = 0$ for a model ultrathin ferromagnetic film with simple cubic crystal structure and monolayer-scale surface roughness. Magnetostatic shape anisotropy favors magnetization in the average surface plane for this geometry. Surface magnetocrystalline anisotropy [10] can either support or oppose this orientational tendency, and both cases are observed frequently in the laboratory [11]. For the present study, we focus exclusively on the case of in-plane magnetization. We also choose a particularly simple, high symmetry, surface morphology. In detail, the film is taken to be a continuous single crystal composed of one complete magnetic layer on a nonmagnetic substrate with a periodic array of square monolayer-height magnetic islands with side length $L$ and center-to-center separation $D$ placed on top (Fig. 1).

Exchange coupling guarantees that atomic moments remain aligned over microscopic distances. For this reason, a *two-dimensional* classical *XY* model with spin lengths $S_i$ proportional to the film thickness at lateral atomic site $i$ will be sufficient for our purposes. The magnetic energy is

$$E = -\sum_{\langle i,j \rangle} J_{ij} \cos(\vartheta_i - \vartheta_j) - a^2 \sum_i K_2^i S_i \cos^2 \vartheta_i$$
$$- a^2 \sum_i K_4^i S_i \cos^2 2\vartheta_i - \mu H \sum_i S_i \cos(\vartheta_i - \varphi),$$
(1)

where the angles $\vartheta_i$ denote the directions of the vector spins $\mathbf{S}_i$ relative to [100], $J_{ij} = J \min[S_i, S_j]^2$ is the
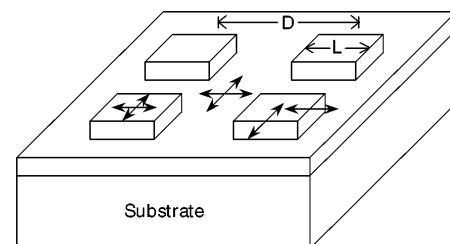


FIG. 1. Schematic view of the rough ultrathin film morphology used in this work. The indicated island geometry is repeated periodically. Arrows indicate local anisotropy axes.

exchange energy between nearest neighbor sites $i$ and $j$, $K_2^i$ and $K_4^i$ specify the strength of twofold and fourfold magnetic surface anisotropies at site $i$, $a$ is the lattice constant, and $\mu = \mu_0 m$, where $m$ is the atomic magnetic moment. The in-plane magnetic field **H** is oriented at an angle $\varphi$ from [100].

We restrict attention here to the case of $\varphi = 0$ [12] and choose the material parameters as $J \sim 10^{-21}$ J, $a = 0.3$ nm, and $m \sim 10^{-23}$ J/T. All sites are assigned a small fourfold anisotropy $K_4 \sim 10^{-2}$ mJ/m$^2$, and, as suggested by the phenomenological Néel model [10], step edges are assigned a uniaxial anisotropy. The latter is chosen here to lay perpendicular [13] to the local step edge with strength $K_2 \sim 1$ mJ/m$^2$. All these numerical values are consistent with recent experiments [14,15].

Unlike most micromagnetic calculations [16], the energy expression Eq. (1) does not include an explicit contribution from magnetostatics. We suggest that this is acceptable in the present case because (i) the effect of shape anisotropy is already included when the planar magnetization we assume is uniform in space, (ii) the magnetostatic contribution to the energy of the nonuniform magnetization distribution within a Néel domain wall is negligible in the ultrathin film limit [6,17], and (iii) it is useful to analyze the effect of competing anisotropies alone so that the effect of reintroducing the dipolar interactions can be appreciated more readily. For example, the atomic-scale discontinuity of the surface height (and hence of the magnetization) at a step edge yields a magnetostatically induced contribution to $K_2$ [18] which breaks the symmetry between parallel and perpendicular anisotropy at the step edges.

The material parameters imply a domain wall width $W \simeq 8\sqrt{J/2K_4} \simeq 200a$, indicating that the magnetization changes exceedingly slowly on the atomic scale. For this reason, large system sizes can be studied by transformation to a representation where the sum over atomic sites in Eq. (1) is replaced by a sum over blocks of aligned spins. We choose square blocks with $b \sim W/20a$ atomic spins per side so that the magnetization changes very little even from block to block. Each block-spin length is rescaled to reflect the local average surface height as before, and the parameters in Eq. (1) are renormalized to guarantee that the new, coarse-grained representation accurately reproduces the original atomic spin representation. One easily checks that the fourfold anisotropy and Zeeman terms each acquire a factor of $b^2$ (all $b^2$ spins per block contribute) while the twofold anisotropy term acquires a factor of $b$ (only the $b$ spins per step that run through the block contribute). The exchange term is unaltered by the blocking transformation [19] as is the anisotropy associated with the island corners.

Zero temperature magnetization reversal is studied by following the local minimum of Eq. (1) as the external field is reversed in small steps from a large positive value

to a large negative value. At each new field, the conjugate gradient method is used to find a local minimum close to the previous local minimum. But when jumps in the magnetization occur, i.e., the minima are not close, the simulation backs up to the configuration before the jump, and relaxation dynamics is used to find the new minimum energy configuration.

For surfaces with no steps, or when the island separation $D$ is small, our model reproduces the Stoner-Wohlfarth result that magnetization reversal occurs by coherent rotation with a coercive field $H_C$ equal to $H_{SW} = 8a^2 K_4/\mu$. The magnitude of $H_{SW}$ ($\sim 5 \times 10^5$ A/m $\sim 2\pi 10^3$ Oe) is about 100 times larger than typical measured coercivities for ultrathin films [7,9,20]. Such a discrepancy between experiment and theory for the coercive field is known as Brown's paradox [21]. It is resolved for bulk samples by invoking the presence of crystalline defects, where local magnetic properties may differ considerably from the average and thus serve as nucleation centers for reversal or pinning sites for pre-existing domain walls [16].

Our calculations support the view that monoatomic steps of single crystal ultrathin films both nucleate rotated domains [6] and impede the motion of domain walls. The reversal process is a combination of nucleation, expansion of domains through morphological constrictions, and coherent rotation within domains. For the geometry studied here, the competition between these processes leads to many types of complex hysteresis loops as a function of island size and separation. Figure 2 shows one characteristic of these loops—the coercive field scaled by $H_{SW}$—for three choices of the island separation $D$. The numerical results accord surprisingly well with simple energy balance arguments [22] that predict four regimes where $H_C/H_{SW}$ varies successively as $W/L$, $LW/D^2$, $W/(D - L)$, and $(D - L + 2W)/D$ as $L/D$ increases.
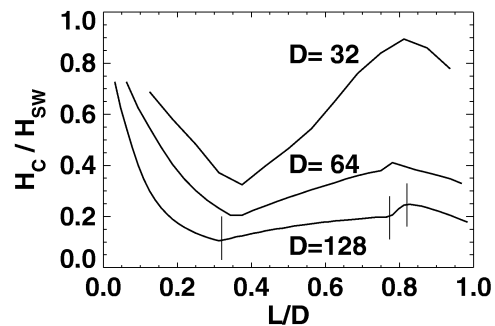


FIG. 2. Coercive field $H_C$ of hysteresis loops obtained upon quasistatic reversal of the external field in (1) with $\varphi = 0$ for the film geometry of Fig. 1 as a function of $L/D$ for different system sizes as labeled. Not shown are the coercivities for $L = 0, 2, D$, for which $H_C = H_{SW}$ in this model. The vertical lines divide the $D = 128$ curve into four regions that are discussed in the text.

As long as $D$ is not so small that $H_C \simeq H_{SW}$, reversal begins with 90° domains nucleated at the edges of each island where the torque, due to the local twofold anisotropy, is largest [23]. Figure 3 shows a stable configuration at remanence where these lens-shaped domains are pinned to the island edges by the energy cost to increase the domain wall length. For small $L/D$, the 90° domains expand as the field is reduced from positive to negative until they "burst" at a field $H_L \propto H_{SW}W/L$. As long as $D - L > L$, the domains expand freely through the channels between the islands until nearly the entire surface is covered. The remaining unrotated spins are confined to regions of area $A \propto LW$ that surround the island edges with anisotropy parallel to the applied field. For very small $L/D$, $H_L$ exceeds the field $H_\perp = 2H_{SW}/3\sqrt{6}$ at which the 90° state is unstable to complete reversal into the 180° state. Accordingly, there is an additional jump in the hysteresis loop when $H_\perp > H_L$. But $H_C = H_L$ nonetheless because the magnetization in the domains is not precisely perpendicular to the **H** axis. There is a small negative component of the magnetization ($M_x = H/H_{SW}$ for small $H$) along the reversed field direction that overcompensates the positive contribution from the unrotated spins noted above.

For fixed $D$, this scenario remains correct as $L$ increases until $H_L$ becomes so small that the negative magnetization of the 90° domains cannot compensate the unrotated edge spins. The hysteresis loop magnetization thus remains positive after its jump at $H = H_L$. The magnetization smoothly passes through zero as the spins in the 90° domains coherently rotate with the applied field. The magnetization is zero when the magnetic field reaches the value $H_R \propto LW/D^2$. The crossover from the first to the second scaling regime in Fig. 2 occurs when $H_L = H_R$.

When $L > D/2$, the channel width is smaller than the island edge length, and the 90° domains between the islands are pinned at the island corners (see Fig. 4). They cannot expand laterally due to the energy cost to create more wall length. Only when the field reaches the value $H_D \propto H_{SW}W/(D - L)$ does a jump in magnetization signal that the domains have squeezed through this morphological constriction. But when $H_D < H_R$, this jump does not affect the coercive field because the postjump magnetization is still positive. Not until $H_D \geq H_R$ does $H_D$ becomes the coercive field. Finally, near layer completion ($L \sim D$) the positive magnetization of the unrotated edge spins can be compensated by rotation of the magnetization in the 90° domains that now do *not* include the narrow channels. The coercive field in this final regime is $H_F \propto H_{SW}(D - L + 2W)/D$.

Magnetization reversal that appears to be closely related to the results reported here has been observed in Kerr microscopy and vector magnetometry experiments reported by Cowburn *et al.* for an ultrathin Ag/Fe/Ag(001) multilayer system [24]. These authors discussed their results using a model that combines the domain wall pinning mechanism of coercivity with a Stoner-Wohlfarth model that features both fourfold and twofold anisotropies. The origin of the uniaxial anisotropy was not specified, but a rather small value of $K_2 \sim 10^{-4}$ mJ/m$^2$ was found to produce the best fit to experiment. Note, however, that this value is assigned (by necessity) to *every* site of the surface in their spatially uniform theory. By contrast, the Néel model [10] and experiments [15] for stepped surfaces suggest a value of $K_2$ that is $10^4$ times larger at step edge sites. We use this larger value but assign it only to step edge sites. Systematic experiments where the step density is varied by changing deposition conditions, coverage, or vicinal miscut will help resolve this matter.

The generalization of the results presented here to the case of an external magnetic field applied at an angle $\varphi \neq 0$, islands with nonsquare shapes and multilevel
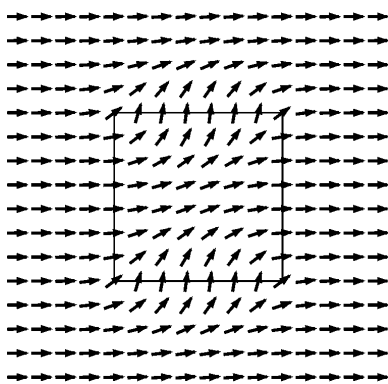
FIG. 3. Spin configuration for $L = 32$, $D = 64$ at the remanent state ($H = 0$). Only every fourth spin block (in each direction) is shown for clarity. The lines indicate the island boundary. This configuration is reproduced periodically in the plane.
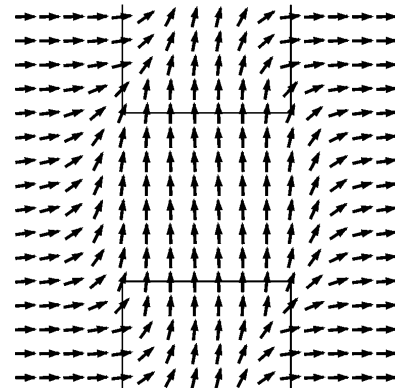
FIG. 4. Spin configuration for $L = 32$, $D = 64$ for $H/H_{SW} = -0.077$. Only every fourth spin block (in each direction) is shown for clarity. The lines indicate the boundaries of two neighboring islands. This configuration is reproduced periodically in the plane.

roughness, is straightforward. Our investigation of these situations, including the effects of magnetostatics, will be reported in full elsewhere [22].

———————

*Present address: Theoretische Tieftemperaturphysik, Gerhard-Mercator-Universität Duisburg, Lotharstrasse 1, D-47408 Duisburg, Germany.

[1] See, e.g, *Ultrathin Magnetic Structures I*, edited by J. A. C. Bland and B. Heinrich (Springer-Verlag, Berlin, 1994); *Ultrathin Magnetic Structures II*, edited by B. Heinrich and J. A. C. Bland (Springer-Verlag, Berlin, 1994).

[2] B. Dieny, J. P. Gavigan, and J. P. Rebouillat, J. Phys. Condens. Matter **2**, 159 (1990); W. Folkerts, J. Magn. Magn. Mater. **94**, 302 (1991).

[3] E. C. Stoner and E. P. Wohlfarth, Philos. Trans. R. Soc. London A **240**, 74 (1948).

[4] J. C. Slonczewski, Phys. Rev. Lett. **67**, 3172 (1991).

[5] I. G. Tringade and P. P. Freitas, J. Appl. Phys. **74**, 2692 (1993).

[6] A. S. Arrott, J. Appl. Phys. **69**, 5212 (1991); A. S. Arrott and B. Heinrich, J. Magn. Magn. Mater. **93**, 571 (1991); A. S. Arrott, in *Nanomagnetism*, edited by A. Hernando (Kluwer, Dordrecht, 1993).

[7] P. Bruno, G. Bayreuther, P. Beauvillain, C. Chappert, G. Lugert, D. Renard, J. P. Renard, and J. Seiden, J. Appl. Phys. **68**, 5759 (1990); M. T. Kief and W. F. Egelhoff, Jr., J. Appl. Phys. **73**, 6195 (1993); Y. L. He and G. C. Wang, J. Appl. Phys. **76**, 6446 (1994); X. Meng, X. Bian, R. Adbouche, W. B. Muir, J. O. Stöm-Olsen, Z. Altounian, and M. Sutton, J. Appl. Phys. **76**, 7084 (1994); F. Baudelet, M.-T. Lin, W. Kuch, K. Meinel, B. Choi, C. M. Schneider, and J. Kirschner, Phys. Rev. B **51**, 12 563 (1995); M. Giesen-Siebert, F. Schmitz, and H. Ibach, Surf. Sci. **336**, 269 (1995).

[8] D. T. Pierce, J. A. Stroscio, J. Unguris, R. J. Celotta, Phys. Rev. B **49**, 14 564 (1994); H. J. Elmers, J. Hauschild, H. Fritzsche, G. Liu, U. Gradmann, and U. Köhler, Phys. Rev. Lett. **75**, 2031 (1995).

[9] B. Heinrich, S. T. Purcell, J. R. Dutcher, K. B. Urquhart, J. F. Cochran, and A. S. Arrott, Phys. Rev. B **38**, 12 879 (1988); A. Berger, U. Linke, and H. P. Oepen, Phys. Rev. Lett. **68**, 839 (1992); J. Chen and J. L. Erskine, Phys. Rev. Lett. **68**, 1212 (1992); W. Weber, C. H. Back, and R. Allenspach, Phys. Rev. B **52**, R14 400 (1995); W. Weber, C. H. Back, A. Bischof, C. Würsch, and R. Allenspach, Phys. Rev. Lett. **76**, 1940 (1996).

[10] L. Néel, J. Phys. Radium **15**, 225 (1954); see also D. S. Chuang, C. A. Ballentine, and R. C. O'Handley, Phys. Rev. B **49**, 15 084 (1994).

[11] U. Gradmann, J. Magn. Magn. Mater. **100**, 481 (1991).

[12] In practice, $\varphi$ is chosen to be a very small positive angle to break the symmetry between the clockwise and counterclockwise senses of magnetization rotation that exists when $\varphi = 0$.

[13] For the Hamiltonian under consideration, parallel and perpendicular uniaxial anisotropy are equivalent. Orienting $\vartheta$ and $\varphi$ from [010] instead of from [100] transforms $K_2$ to $-K_2$ while leaving Eq. (1) otherwise unchanged.

[14] B. Heinrich and J. F. Cochran, Adv. Phys. **42**, 523 (1993).

[15] M. Albrecht, T. Furubayashi, M. Przybylski, J. Koreki, and U. Gradmann, J. Magn. Magn. Mater. **113**, 207 (1992).

[16] H. N. Bertram and J.-G. Zhu, in *Solid State Physics*, edited by H. Ehrenreich and D. Turnbull (Academic, Boston, 1992), Vol. 46, pp. 271–371; M. Mansuripur, *The Physical Principles of Magneto-Optical Recording* (Cambridge University Press, Cambridge, England, 1995).

[17] H. Riedel and A. Seeger, Phys. Status Solidi **46**, 377 (1971).

[18] J.-G. Zhu (private communication).

[19] See, e.g., M. Bander and D. L. Mills, Phys. Rev. B **38**, 12 015 (1988).

[20] C. M. Schneider, P. Bressler, P. Schuster, J. Kirschner, J. J. de Miguel, and R. Miranda, Phys. Rev. Lett. **64**, 1059 (1990); P. Krams, F. Lauks, R. L. Stamps, B. Hillebrands, and G. Güntherodt, Phys. Rev. Lett. **69**, 3674 (1992).

[21] A. Aharoni, Rev. Mod. Phys. **34**, 227 (1962).

[22] R. A. Hyman, A. Zangwill, M. D. Stiles, and L.-H. Tang (unpublished).

[23] Similar effects in small magnetic particles are reported in D. A. Dimitrov and G. M. Wysin, Phys. Rev. B **50**, 3077 (1994); D. A. Dimitrov and G. M. Wysin, Phys. Rev. B **51**, 11 947 (1995); K. Zhang and D. R. Fredkin, J. Appl. Phys. **79**, 5762 (1996).

[24] R. P. Cowburn, S. J. Gray, J. Ferré, J. A. C. Bland, and J. Miltat, J. Appl. Phys. **78**, 7210 (1995).